Supplementary information

Non-invasive quantitative chemical measurements of liposomal formulations using Raman spectroscopy

Elizabeth J. Legge,[a] Ryan T. Coones,[a] William A. Lee,[a] Yiwen Pei,[a] Natalie A. Belsey,[a,b] Caterina Minelli[a*]

a. National Physical Laboratory, Teddington TW11 0LW, U.K.
b. School of Chemistry & Chemical Engineering, University of Surrey, Guildford GU2 7XH, UK

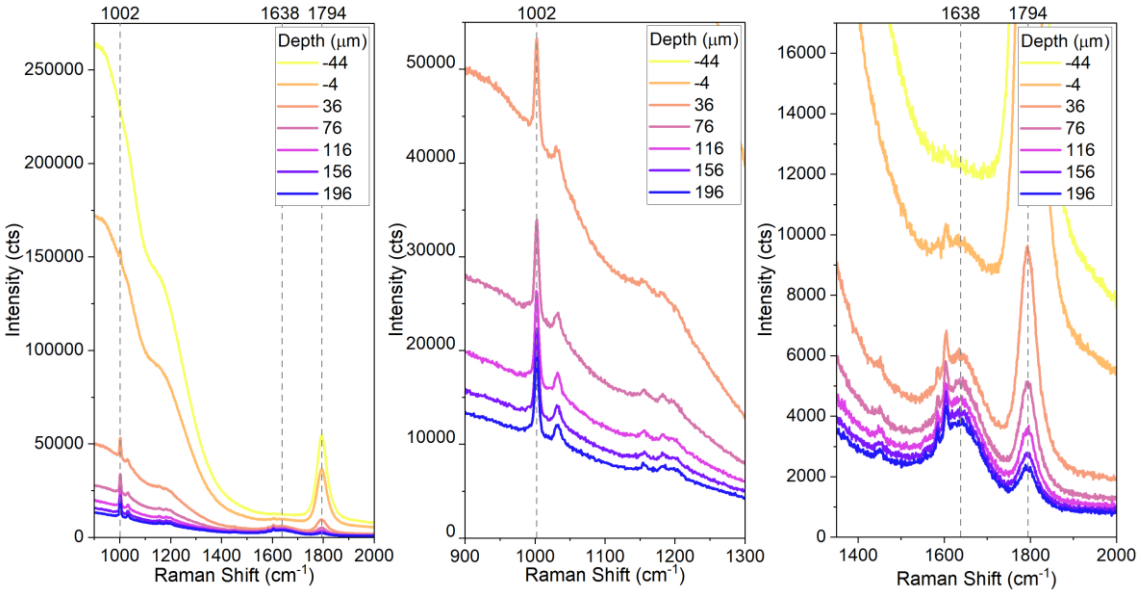

Figure S1 (a) Raman spectra at different points in a depth profile measurement of 200 nm polystyrene (PS) particles in ultrapure water in a glass vial, before any baseline subtraction was performed. (b) A zoomed in region of (a) containing the PS peak at 1002 cm^{-1}. (c) A zoomed in region of (a) containing the water peak at 1638 cm^{-1}. Depth positions have been set so that a depth of 0 μm is at the interface between the glass vial and PS solution.

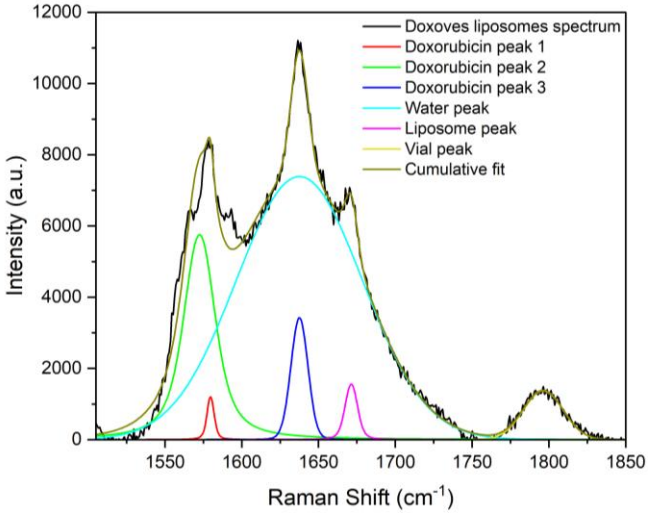

Figure S2 Peak fit of the water peak in a Doxoves® liposomes spectrum, where other contributions are from the vial, liposomes, and doxorubicin.

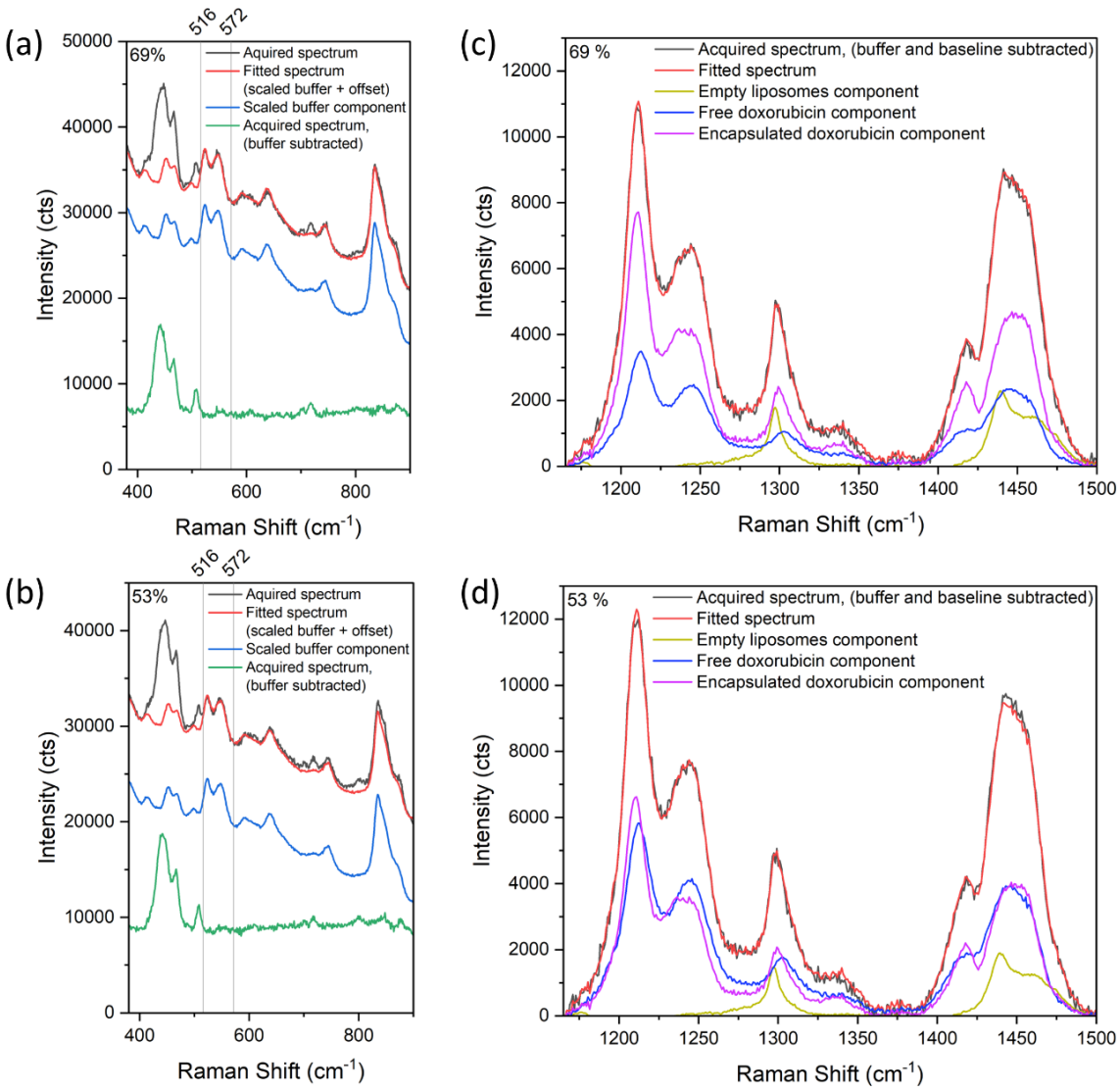

Figure S3 Examples of a fit of the Raman spectrum from the buffer sample to the Raman spectrum of a sample containing liposomes, doxorubicin HCl and buffer, where the example spectra are a mixture of Doxoves® and free doxorubicin, at a measured encapsulation efficiency of (a) 69 % (expected 66 %) and (b) 53 % (expected 51 %). The buffer spectrum (plus an offset value) has been scaled to fit the sample spectrum between 516-572 cm^{-1}, a region in which there are no overlapping peaks with the doxorubicin HCl or liposomes spectra. The fitted buffer component was subsequently subtracted from the Raman spectrum of the liposomal (and/or doxorubicin) sample, after which a linear baseline was subtracted between 1165-1505 cm^{-1}. Example fitting of the Raman spectrum from the 100 % encapsulated, 0 % encapsulated (100 % free), and plain control liposomes samples to the combined samples (all spectra have had the buffer component subtracted using the method in (a) and (b), and a linear baseline subtracted), with the resulting peak intensities used to calculate an encapsulation efficiency of (c) 69 % (expected 66 %) and (c) 53 % (expected 51 %). The fitting in (c) and (d) was performed between 1180-1320 cm^{-1} to focus on the doxorubicin and lipid peaks.

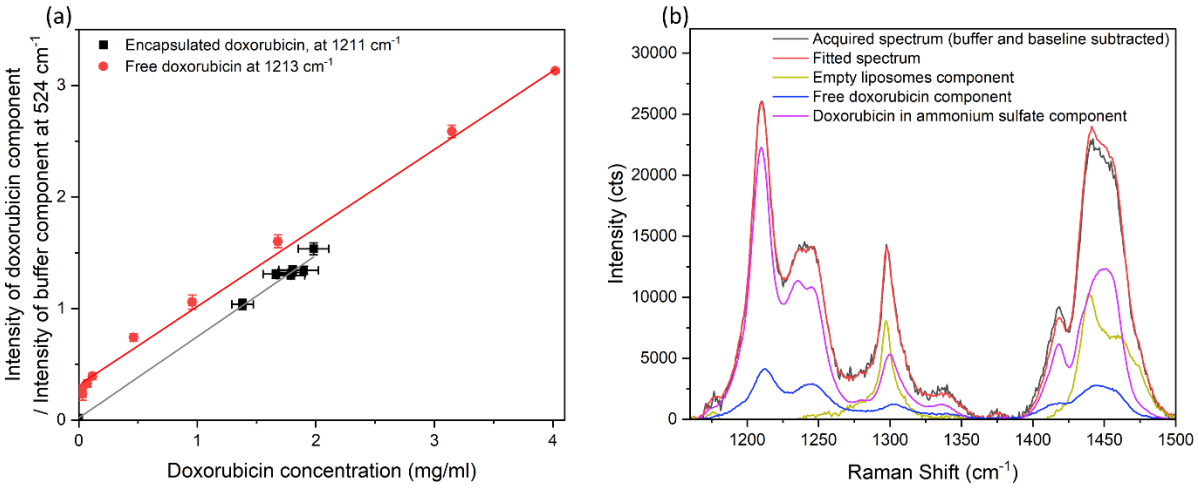

Figure S4 (a) Height intensity ratio of the doxorubicin component measured at 1211-1213 cm^{-1} and the buffer component measured at 524 cm^{-1}. Each point is the average value from 3 analysed spectra, and the error bars are the standard deviation. (b) Example fitting of the Raman spectrum from doxorubicin in ammonium sulphate, 0 % encapsulated (100 % free), and plain control liposomes samples to the 100% encapsulated sample (spectrum has had the buffer component subtracted and a linear baseline subtracted), with the resulting peak intensities used to form calibration curves of the encapsulated and free doxorubicin concentrations in (a). The fitting in (b) was performed between 1180-1320 cm^{-1} to focus on the doxorubicin and lipid peaks. The acquisition time for 3 samples with a free doxorubicin concentration of <0.15 mg/ml (>94 % encapsulated) was increased to 4 accumulations of 90 s in order to detect small changes, whereas all other samples were measured with 2 accumulations of 60 s.

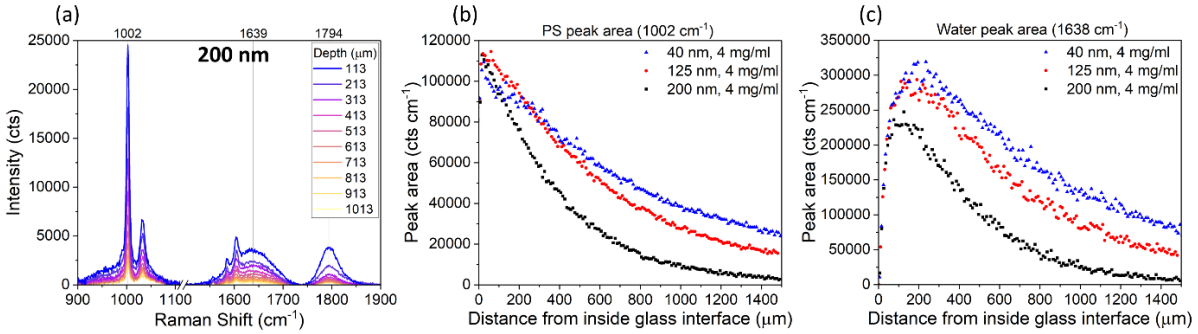

Figure S5 (a) Raman spectra at different points in a depth profile measurement of 200 nm polystyrene (PS) particles in ultrapure water in a glass vial. Area of the peak in the Raman spectrum of 40 nm, 125 nm, and 200 nm PS samples for (b) the PS peak at 1002 cm^{-1} and (c) the water peak at 1638 cm^{-1}, measured at different depths inside the glass vial. Depth positions have been set so that a depth of 0 μm is at the interface between the glass vial and PS solution.

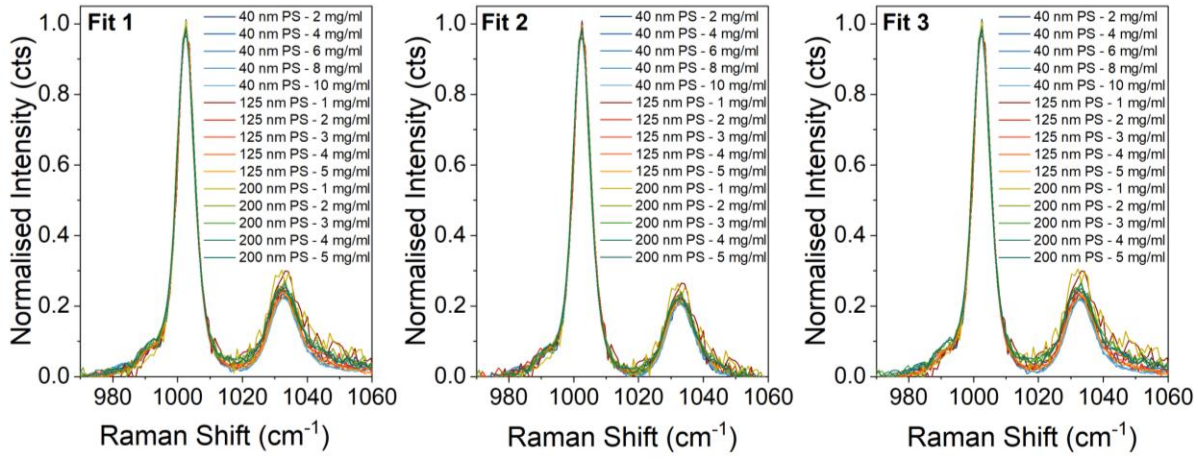

Figure S6 Raman spectra of 40 nm, 125 nm and 200 nm PS in water, at a concentration of 1-10 mg/ml, after baseline subtraction around the 1002 cm^{-1} PS peak, where a linear baseline was fitted between (a) 950 cm^{-1} and 1090 cm^{-1}, (b) 970 cm^{-1} and 1055 cm^{-1} and (c) 930 cm^{-1} and 1080 cm^{-1}. All spectra are normalised to the height of the fitted PS peak at 1002 cm^{-1}, to compare differences in peak shape after baseline subtraction.

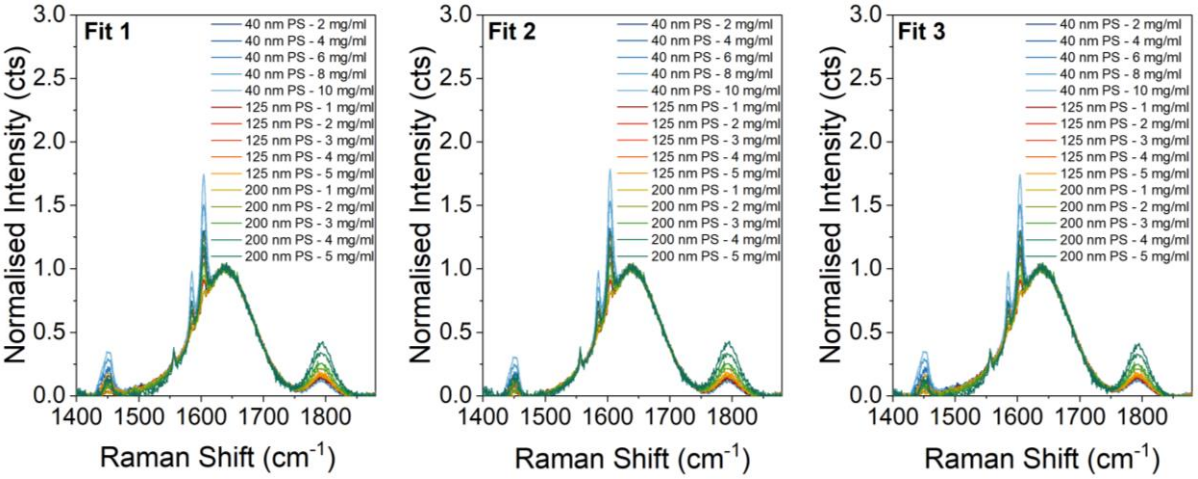

Figure S7 Raman spectra of 40 nm, 125 nm and 200 nm PS in water, at a concentration of 1-10 mg/ml, after baseline subtraction around the 1638 cm^{-1} water peak, where a linear baseline was fitted between (a) 1420 cm^{-1} and 1860 cm^{-1}, (b) 1485 cm^{-1} and 1860 cm^{-1} and (c) 1410 cm^{-1} and 1845 cm^{-1}. All spectra are normalised to the height of the fitted water peak at 1638 cm^{-1}, to compare differences in peak shape after baseline subtraction.

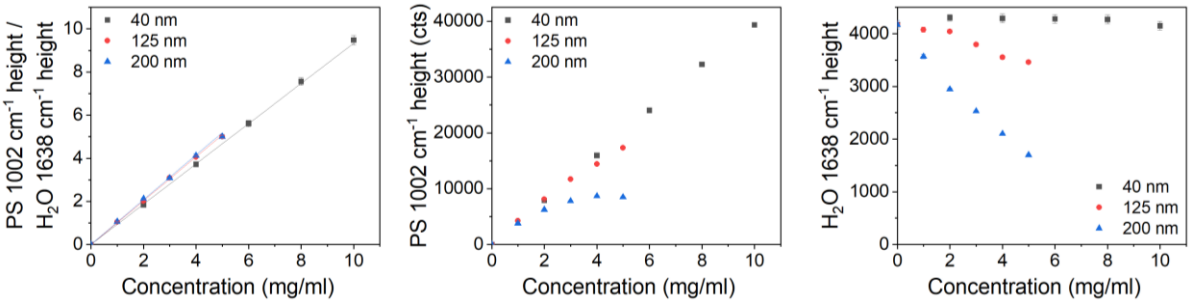

Figure S8 (a) Ratio of the height of the fitted peaks in the Raman spectra at 1002 cm^{-1} and 1638 cm^{-1}, for samples containing different sizes and concentrations of PS. Each point on the graph is an average of 3 spectra, acquired at different places (but the same depth of 460 µm) through the vial. Three different methods of baseline subtraction were investigated for each peak (Figure S6 and S7), with the most consistent method chosen to calculate the peak height. The error bars represent the standard deviation of the fitted areas from each baseline subtraction method. A linear curve was fitted to each data set in (a). (b) Peak height intensity of the PS (1002 cm^{-1}) peak. (c) Peak height intensity of the ultrapure water (1638 cm^{-1}) peak. Corresponding data on peak areas are in the main manuscript (Figure 3).

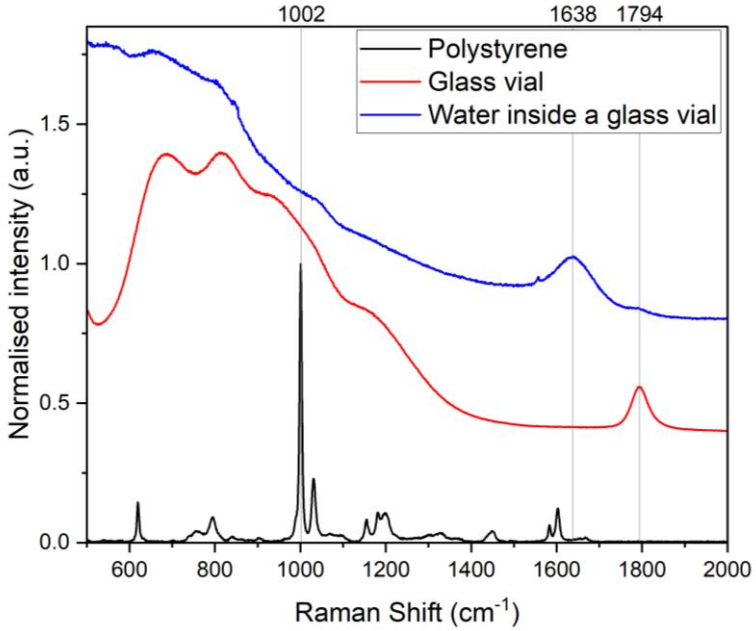

Figure S9 Example Raman spectra of polystyrene, the wall of an empty glass vial, and water inside a glass vial. The main peaks used for analysis in this work have been labelled.

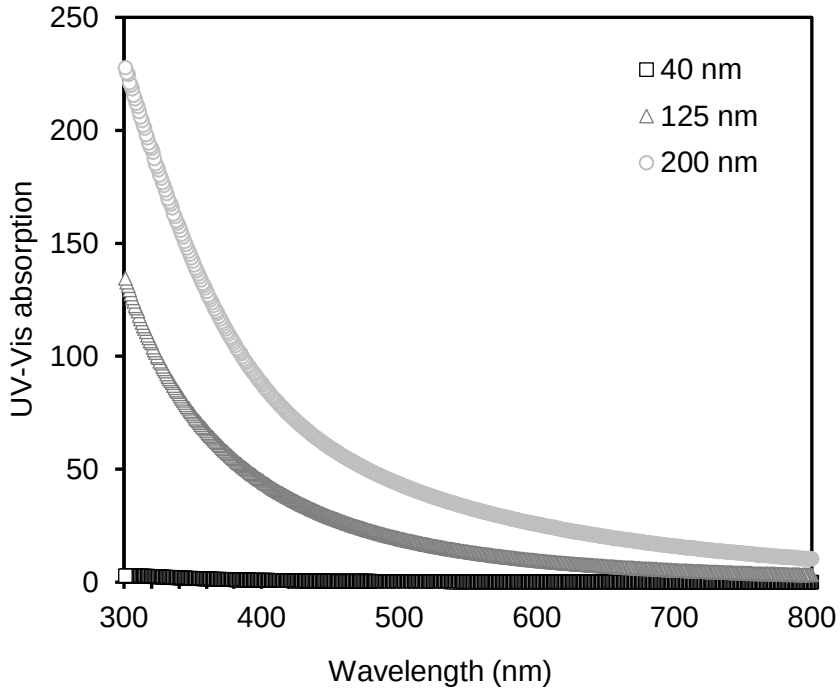

Figure S10 UV-vis absorption spectra of PS particles with a size of 40 nm, 125 nm and 200 nm. The spectra were scaled to be representative of the same mass concentration for all samples.

Table S 1 Theoretical values of 40 nm, 125 nm and 200 nm PS sizes, calculated from the nominal particle sizes.

Particle size (nm)	Radius (m)	Volume (m^3)	Volume of water displaced by one particle (ml)	Mass (g)
40	2.00×10^{-8}	3.35×10^{-23}	3.35×10^{-17}	3.53×10^{-17}
125	6.25×10^{-8}	1.02×10^{-21}	1.02×10^{-15}	1.08×10^{-15}
200	1.00×10^{-7}	$4.19 \times 10E^{-21}$	4.19×10^{-15}	4.41×10^{-15}

Table S 2 Number of particles and resulting volume of water in the sample after displacement from the particles. Information is calculated from the nominal concentrations for the 200 nm particles.

Concentration (mg/ml)	Number of particles per ml	Volume of water displaced per ml (ml)	Volume of water per ml (ml)	Volume fraction of water (%)
1	2.27E+11	0.0010	0.9990	99.90
2	4.54E+11	0.0019	0.9981	99.81
3	6.81E+11	0.0029	0.9971	99.71
4	9.08E+11	0.0038	0.9962	99.62
5	1.13E+12	0.0048	0.9952	99.52

Table S 3 Number of particles and resulting volume of water in the sample after displacement from the particles. Information is calculated from the nominal concentrations for the 125 nm particles.

Concentration (mg/ml)	Number of particles per ml	Volume of water displaced per ml (ml)	Volume of water per ml (ml)	Volume fraction of water (%)
1	9.30E+11	0.0010	0.9990	99.90
2	1.86E+12	0.0019	0.9981	99.81
3	2.79E+12	0.0029	0.9971	99.71
4	3.72E+12	0.0038	0.9962	99.62
5	4.65E+12	0.0048	0.9952	99.52

Table S 4 Number of particles and resulting volume of water in the sample after displacement from the particles. Information is calculated from the nominal concentrations for the 40 nm particles.

Concentration (mg/ml)	Number of particles per ml	Volume of water displaced per ml (ml)	Volume of water per ml (ml)	Volume fraction of water (%)
2	5.67E+13	0.0019	0.9981	99.81
4	1.13E+14	0.0038	0.9962	99.62
6	1.70E+14	0.0057	0.9943	99.43
8	2.27E+14	0.0076	0.9924	99.24
10	2.84E+14	0.0095	0.9905	99.05

Measurement of liposome diameter using MADLS and PTA

Liposomes were dispersed in a buffer solution (10 % w/v sucrose, 10 mM histidine, pH 6.5) and the particle diameter was measured using both multi-angle dynamic light scattering (MADLS) and particle tracking analysis (PTA). Both measurements yield information about the particle diameter and both techniques gave consistent results showing a monodisperse liposome population. For MADLS, the particle diameter was determined through the combination of DLS measurements performed at three different angles – 173 °, 90 °, and 17 °. Measurement of the Doxoves® sample by MADLS gave an intensity-based particle size diameter of 92.7 ± 1.4 nm. The Doxoves® as measured by PTA was 93 ± 15 nm, in good agreement with the product certificate (94.7 ± 1.0 nm). Representative number-based particle size distributions are shown in Figure S11.

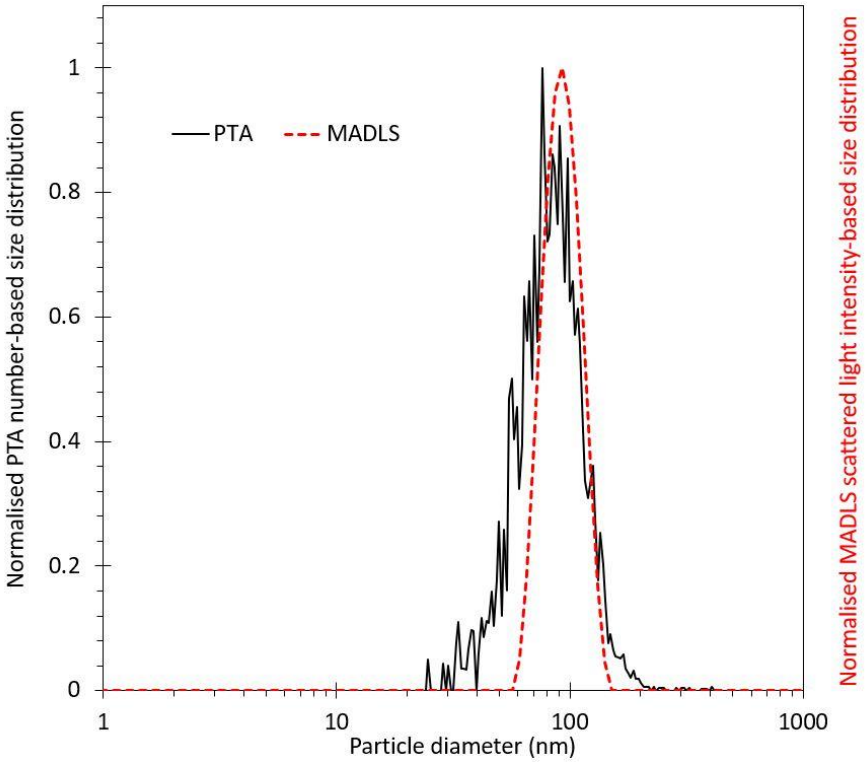

Figure S11 Representative number-based particle size distributions for PTA (solid black line) and scattered light intensity based for MADLS (dashed red line) showing a monomodal distribution of liposomes with a mode diameter of 93 nm. Samples were diluted in a buffer (10 % w/v sucrose, 10 mM histidine, pH 6.5).

Calibration for measurement of number concentration of nanoparticles

PTA measurements were utilised to provide information on particle size of a loaded liposomal sample to validate MADLS measurements. A representative size and size distribution of the loaded liposome suspension can be found in Figure S11. A monomodal size distribution was observed in this sample, suggesting no degree of agglomeration was detected. The number concentration for liposomal samples provided some challenges in terms of the ability to visualise and detect the particles given that they are weak scatterers. As a result of the lower-than-expected scattering, the PTA tracking algorithm was under-reporting the number of particles that were detected and counted compared to both the nominal certificate value and the MADLS number concentration by 2 orders of magnitude. The number concentration as measured by MADLS was (1.06 ± 0.04) x10^{13} p/mL.

Ultraviolet-visible (UV-vis) spectroscopy and Fluorescence spectroscopy

In the case of the UV-visible absorption spectra (Figure S12), a scattering component contributed to the liposomes spectrum of the form $y = A + \frac{B}{\lambda^4}$, where *A* is a constant that describes the y-offset of the scattering curve, and *B* describes the amplitude and shape of the curve[45]. In this case, the scattering component was fit to the measured Doxoves® absorption spectrum using a sum of least squares, where the fit was constrained such that the subtracted spectrum did not have any negative absorption values. In this regard, there is no unique solution to the scattering component that was subtracted for any given spectrum, and thus some variability in the scattering-subtracted Doxoves® spectrum can be expected.

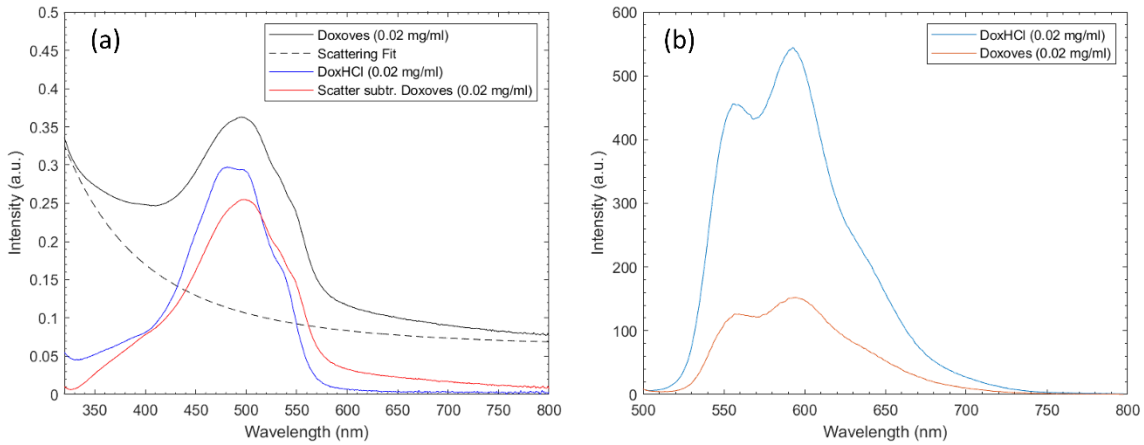

Figure S12 (a) UV-vis absorption spectra of Doxoves (0.02 mg/ml, solid black line), doxorubicin hydrochloride (DoxHCl, 0.02 mg/ml, blue line), a calculated scattering component of the spectrum from the liposome contribution (dashed black line), and the Doxoves spectrum with the scattering component subtracted (0.02 mg/ml, red line). (b) shows the fluorescence emission spectra of the Doxoves formulation (0.02 mg/ml, orange line) and doxorubicin HCl at the same doxorubicin concentration (0.02 mg/ml, blue line).

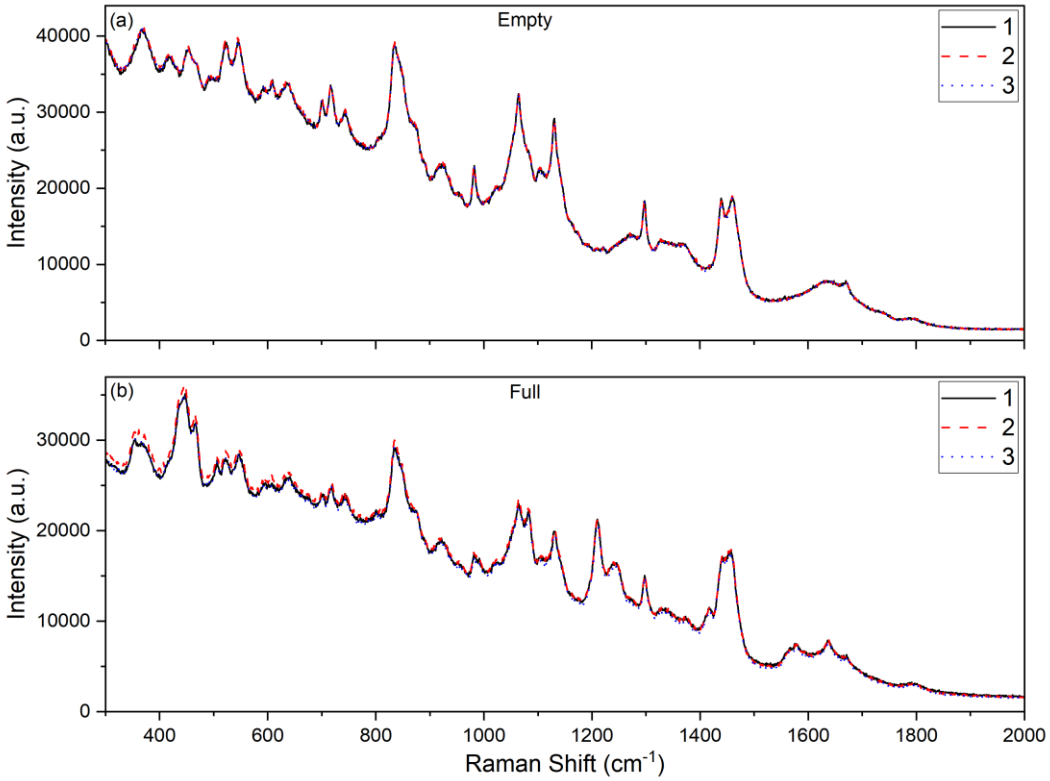

Figure S13 Raman spectra of (a) empty liposomes and (b) liposomal doxorubicin (Doxoves®), where repeat measurements have been acquired on the same sample, in sequence, in the order labelled.

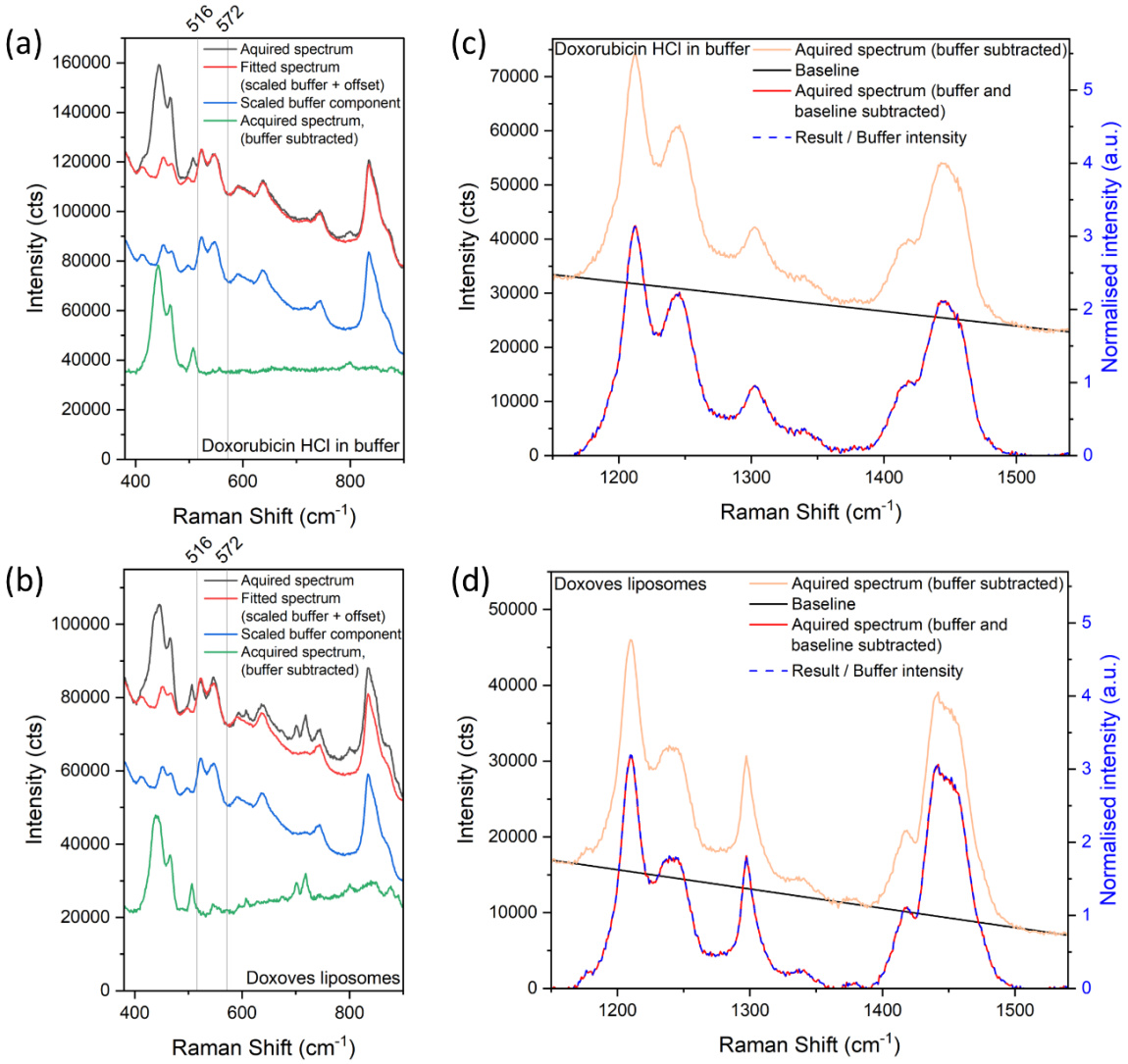

Figure S14 Examples of a fit of the Raman spectrum from the buffer sample to the Raman spectrum of a sample containing (a) doxorubicin HCl in buffer, and (b) Doxoves® liposomes. The buffer spectrum (plus an offset value) has been scaled to fit the sample spectrum between 516-572 cm^{-1}, a region in which there are no overlapping peaks with the doxorubicin HCl or liposomes spectra. The fitted buffer component was subsequently subtracted from the Raman spectrum of the liposomal (and/or doxorubicin) sample, after which a linear baseline was subtracted between 1165-1505 cm^{-1}. Example fitting and subtraction of the linear baseline to the Raman spectrum of (c) doxorubicin HCl in buffer, and (d) Doxoves® liposomes (both spectra have had the buffer component subtracted using the method in (a) and (b)). The spectrum in (c) and (d) was then normalised to the height intensity of the scaled buffer peak in (a) and (b) at 524 cm^{-1} (after baseline subtraction).

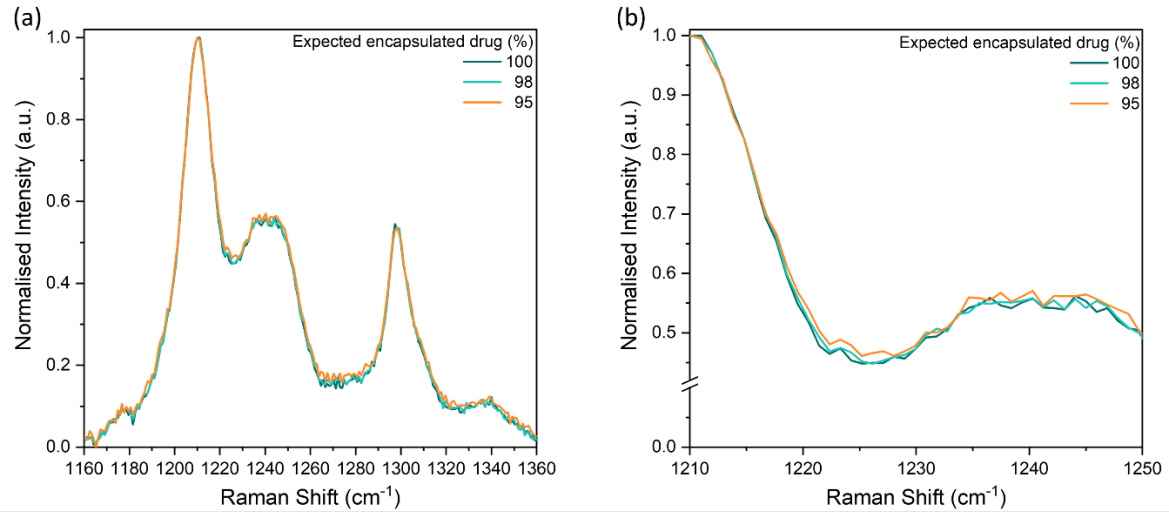

Figure S15 (a) Raman spectrum of samples containing a combination of free and encapsulated doxorubicin, after subtraction of the buffer component, baseline subtraction, and normalisation between 0 and 1. (b) The same spectra as in (a) showing a smaller range of values, to aid visualisation of the differences.